Heat Dissipation for Au Particles in Aqueous Solution: Relaxation Time versus Size

Min Hu and Gregory V. Hartland*

Department of Chemistry and Biochemistry, 251 Nieuwland Science Hall, University of Notre Dame, Notre Dame, Indiana 46556-5670

Received: March 1, 2002; In Final Form: April 25, 2002

The rate of energy dissipation from Au nanoparticles to their surroundings has been examined by pump−probe spectroscopy. These experiments were performed for particles suspended in aqueous solution, with average sizes ranging from 4 to 50 nm in diameter. The results show that energy relaxation is a very nonexponential process. Fitting the data to a stretched exponential function yields a characteristic time scale for relaxation that varies from ca. 10 ps for the smallest particles examined (∼4 nm diameter) to almost 400 ps for the 50 nm diameter particles. The relaxation times are proportional to the square of the radius, but do not depend on the initial temperature of the particles (i.e., the pump laser power). For very small particles, the time scale for energy dissipation is comparable to the time scale for electron−phonon coupling, which implies that significant energy loss occurs before the electrons and phonons reach thermal equilibrium within the particle.

Introduction

The interaction of light with metal nanoparticles has received a large amount of attention in the past decade; for recent reviews, see refs 1−5. The canonical picture of the photophyics of these systems is that light excites electrons, which subsequently relax by electron−electron (e−e) scattering to give a hot electron distribution. The hot electrons then equilibrate with the lattice by electron−phonon (e−ph) coupling. This sequence of events is identical to what happens in bulk metals.[6,7] In bulk metals, the energy deposited by the laser diffuses away from the excitation region in a way that depends on the thermal conductivity of the metal. In contrast, for particles, the final step in the relaxation process is transfer of energy from the hot electron/phonon system to the environment.[1,2] Most of the recent experimental work in this area has focused on the relatively fast e−e and e−ph relaxation processes. However, the particle-to-surroundings energy transfer process is also important and is not very well understood. This process is the rate determining step for energy dissipation; that is, it controls how long the particles remain hot after laser excitation. Our interest in energy transfer from the particles to their environment stems from studying laser-induced alloying in core−shell bimetallic particles.[8] To calculate an effective interdiffusion time for these systems we need to know how long the particles remain hot after excitation, which means we need to know the time scale for energy transfer to the environment.

Typical time scales quoted in the literature for energy dissipation from metal particles are several hundred picoseconds.[1,2,9,10] However, it is not clear how this process depends on factors such as the size and surface properties of the particles. In recent studies, El-Sayed and co-workers examined how the time scale for energy dissipation from ∼15 nm Au particles depended on the environment.[11,12] Their results showed that the surroundings influence relaxation, specifically, liquids with higher thermal conductivities give faster relaxation times.[11] Au particles in $MgSO_4$ powder were also examined, again they found that the relaxation time depends on the environment of the particles.[12] In this paper, we present results for different sized Au particles in aqueous solution. The aim of these experiments is to determine how size affects the rate of heat dissipation. The particles are stabilized by weakly adsorbed simple anions (such as citrate or chloride), so we do not expect surface chemistry to play a role in the relaxation process. As expected, our results show that smaller particles relax faster because of their larger surface-to-volume ratio. We have attempted to model the relaxation process using a classical expression for heat dissipation from a sphere.[13] The results of these calculations are only in qualitative agreement with the experimental results. We attribute the differences to approximations made in defining the boundary conditions for the calculations. Although our experimental results cannot be quantitatively analyzed, they do allow us to draw some general conclusions about the energy relaxation process. Specifically, the time constant for relaxation is proportional to the surface area of the particles, and is independent of the initial temperature, at least in the temperature range examined in these experiments.

In addition, we will show that for very small particles (∼4 nm diameter) the time scale for energy transfer to the environment is competitive with the time scale for e−ph coupling. Thus, particles in this size regime do not achieve equilibrium between the electrons and phonons before they interact with their environment. These particles provide an opportunity to observe interactions between hot electrons and the solvent that surrounds the particles.[14] The results reported here are relevant to experiments where laser induced heating is used to change the shape or structure of metal particles[8,15−19] and to temperature jump experiments where heat dissipation from metal particles is employed to cause a macroscopic increase in the temperature of a sample.[20] Our results are also pertinent to studies of the optical limitation effects of metal particles.[21,22]

* To whom correspondence should be addressed. E-mail: hartland.1@nd.edu. Fax: (219) 631-6652.

10.1021/jp020581+ CCC: $22.00
Published on Web 06/21/2002

Apparatus and Techniques

The experiments described in this paper were performed with a regeneratively amplified Ti:sapphire laser. Briefly, the output of the laser (λ = 780 nm; 0.5 mJ/pulse; 120 fs fwhm sech^2 deconvolution; 1 kHz repetition rate) was split by a 90:10 beam splitter. The 90% portion was frequency doubled in a 1 mm BBO crystal to generate 390 nm pump pulses. The intensity of these pulses was controlled with a λ/2-waveplate/polarizer combination. The 10% portion was used to generate a white light continuum in a 3 mm sapphire window, which was used as the probe. The pump and probe were crossoverlapped at the sample by focusing with a 10 cm lens, and the polarizations were set to parallel for all of the experiments described below. Specific probe wavelengths were selected using a Jobin-Yvon Spex H-10 monochromator (10 nm spectral resolution) placed after the sample. Fluctuations in the probe laser intensity were normalized by splitting-off and monitoring a small portion of the probe beam before the sample. The timing between the pump and probe pulses was controlled by a stepper motor driven translation stage (Newport UTM150PP.1). This translation stage and the geometry of our experiment allow us to collect transient absorption data over an approximately 500 ps delay range.

The pump laser intensity at the sample was measured by a Molectron J3−02 Energy Detector, and the pump laser spot size was $(6 \pm 1) \times 10^{-4}$ cm^2 for these experiments. The spot size was measured using both standard laser burn paper and by observing the laser-induced color change in a thin film of Au particles deposited on a glass slide. These measurements gave equivalent results, but the images of the beam are much clearer from the thin Au particle films.

Au particles with a 15 nm diameter were prepared using the standard citrate reduction recipe.[23] Smaller 4 nm diameter Au particles were made using $NaBH_4$ as the reductant rather than citrate. Particles with 26, 40, and 50 nm diameters were made by depositing Au onto the surface of the 15 nm particles using radiation chemistry.[24,25] In this technique, the excess citrate is removed by ion exchange with Cl^-, and γ irradiation is carried out under an atmosphere of nitrous oxide with ~0.3 M methanol added to the solution. Thus, the 15 nm particles are stabilized by adsorbed citrate ions, the 4 nm particles are (probably) stabilized by BO_2^- (the oxidized form of BH_4^-), and the larger particles prepared by radiation chemistry are stabilized by Cl^-. These different anions are not expected to significantly change the energy relaxation dynamics. The particle sizes were measured either by TEM or by observed quantum beats due to the symmetric breathing mode of the particles in transient absorption experiments.[26,27] The samples were held in 2 mm cuvettes, and the experiments were performed without flowing. However, the relatively low pump laser powers and repetition rates used in these experiments mean that thermal effects, which arise from heat accumulation in the solvent, are not a problem. The concentration of Au was adjusted to $\sim 1.2 \times 10^{-4}$ M for all of the experiments presented below. The probe laser wavelength used was λ = 530 nm, i.e., at the maximum of the Au plasmon band. This wavelength was chosen for several reasons. First, tuning the probe to the maximum of the plasmon band maximizes the signal intensity, which allows us to perform experiments at low excitation levels. Second, the contribution from the beat signal mentioned above is minimized at this wavelength.[28] Third, the signal in this spectral region is dominated by the broadening of the plasmon band induced by the increase in the electronic temperature.[29−31] This creates a transient bleach at the plasmon band maximum, the magnitude of which tracks the electronic temperature.[29,30] The transient absorption signals at wavelengths significantly displaced from the plasmon band maximum have a more complicated temperature dependence.[30]

Careful measurement of the power absorbed by the sample shows that the pump laser absorption follows Beer's law under our experimental conditions. In this case, the temperature rise in the particles can be simply calculated from the pump laser intensity (I_0), the spot size (σ), the sample absorbance (A), and the concentration and heat capacity (C_p) of Au:

$$\Delta T = \frac{I_0(1-\zeta)^2(1-10^{-A})}{C_p[\mathrm{Au}]\sigma l} \qquad (1)$$

In this equation, the $(1-\zeta)^2$ factor accounts for scattering of the pump laser at the front and back surfaces of the input window of the sample cell ($\zeta \approx 0.04$) and l is the length of the cell. Equation 1 assumes that no energy is lost to the environment during the e−ph coupling process. We will show below that this is a reasonable assumption for ultrafast experiments with particles larger than ca. 10 nm diameter. Note that the temperature increase in the particles primarily depends on the heat capacity of Au, the absorption coefficient of the particles at the pump laser wavelength, and the pump laser flux (I_0/σ) at the sample. In addition, for 390 nm pump pulses, the absorption coefficient is $\epsilon \approx 2000$ M^{-1} cm^{-1} for all of the samples examined, i.e., ϵ does not strongly depend on size at this wavelength.[24,25] Also note that under the conditions of our experiments ($<\mu$J pulse energies) the temperature increases created by the pump laser are <200 °C. The error in the calculated temperatures from eq 1 is ±15% and is almost completely due to the uncertainty in the laser spot size.

Theory for Heat Dissipation from a Sphere

The situation we are interested in, heat transfer from a sphere to an infinite medium, is a classic problem in mechanical engineering.[32] The heat transfer equations that govern the temperatures of the sphere and its surroundings are[13,32]

$$\frac{\partial T_p}{\partial t} = \frac{\alpha_p}{r}\frac{\partial^2}{\partial r^2}[rT_p(r,t)], \quad \frac{\partial T_s}{\partial t} = \frac{\alpha_s}{r}\frac{\partial^2}{\partial r^2}[rT_s(r,t)] \qquad (2)$$

where the subscript "p" refers to the particle, "s" refers to the solvent, and α is the thermal diffusivity of the particle or the solvent. α is related to the thermal conductivity k by $\alpha = k/\rho C_p$, where ρ is the density and C_p is the heat capacity. Explicit solutions to these equations are given in ref 13 for the boundary conditions that at the interface ($r = R$) the temperature and heat flux are equal for the particle and the solvent, i.e., $T_p[R,t] = T_s[R,t]$ and $k_p(\partial T_p/\partial r)_{r=R} = k_s(\partial T_s/\partial r)_{r=R}$ where k_i is the thermal conductivity of the solvent or the particle. The initial conditions used are that the temperature profiles in the particle and the solvent are uniform (but different) at $t = 0$.

Plots of the temperature inside the particle using the general solution to the heat transfer equations (eq 13 of ref 13) are shown in Figure 1 for different diameter particles, with an initial temperature increase of 80 K. The values of the parameters used are k_p = 317 W m^{-1} K^{-1}, k_s = 0.611 W m^{-1} K^{-1}, C_p(Au) = 129 J g^{-1} K^{-1}, $C_p(H_2O)$ = 4.18 J g^{-1} K^{-1}, ρ(Au) = 19.3 g cm^{-3}, and $\rho(H_2O)$ = 1.0 g cm^{-3}.[33,34] The only adjustable parameter in these calculations is the point in the sphere where the temperature is evaluated: we have chosen to use $r = 2R/3$. The exact value of r is not critical, as long as it is not $r = 0$ or R.

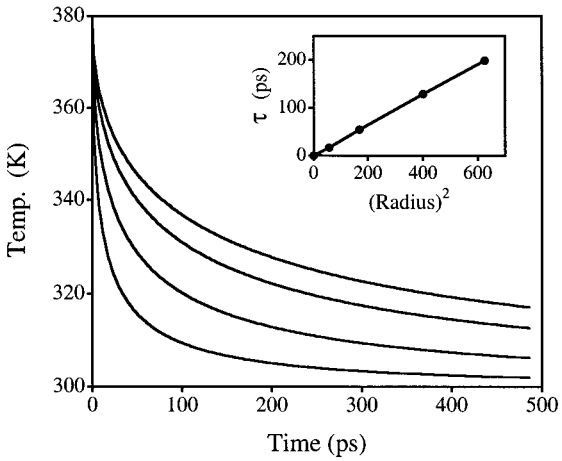

Figure 1. Calculated temperature versus time profiles using eq 13 from ref 13. From top to bottom, the different traces correspond to particles with diameters of 50, 40, 26, and 15 nm. The insert shows the characteristic time constant for energy dissipation (τ) obtained from fitting the temperature profiles to eq 3, plotted against the square of the radius (in nm^2).

The calculations show that heat dissipation from the particles does not follow a single (or even double) exponential decay. The temperature versus time profiles can be conveniently fitted using a stretched exponential function:

$$F(t) = A\, e^{-(t/\tau)^{\beta}} \tag{3}$$

This function was chosen simply for convenience: it is a very flexible function that allows us to define a characteristic time scale for energy dissipation. The values of the time constant τ obtained by fitting the calculated temperature profiles to eq 3 are plotted versus the square of the radius in the insert of Figure 1. This plot shows that the characteristic time scale for energy dissipation $\tau \propto R^2$; that is, τ is proportional to the surface area of the particles. Note that the stretching parameter β obtained from the fit changes from $\beta = 0.35$ for the 15 nm particles to $\beta = 0.44$ for the 50 nm particles. It is also important to note that the form of the temperature profile for a given size particle is independent of the initial temperature: τ and β do not change with ΔT. This is a rather unexpected result from these calculations (at least for us), and it will be directly tested in the experiments described below.

Experimental Results and Discussion

Figure 2 shows typical transient bleach data obtained for 15 nm diameter particles with 0.2 μJ pump pulses and a probe laser wavelength of $\lambda = 530$ nm. For a given sample and pump laser power, the magnitude of the bleach signal is roughly proportional to the temperature of the electron distribution.[29,30] The data shows two distinct regions: (i) an initial fast decay due to coupling between the hot electrons created by the pump laser and the phonon modes (labeled as e−ph coupling in Figure 2) and (ii) a slow decay due to heat dissipation from the particle to the environment (labeled as ph−ph coupling). When the time scale for ph−ph coupling is much longer than the time scale for e−ph coupling, the break in the curve in Figure 2 represents the point where the electrons and phonons have reached equilibrium. At this point, the temperature of the particle is given by eq 1.

Transient bleach data for different sized Au particles are presented in Figure 3. The pump laser powers used in these

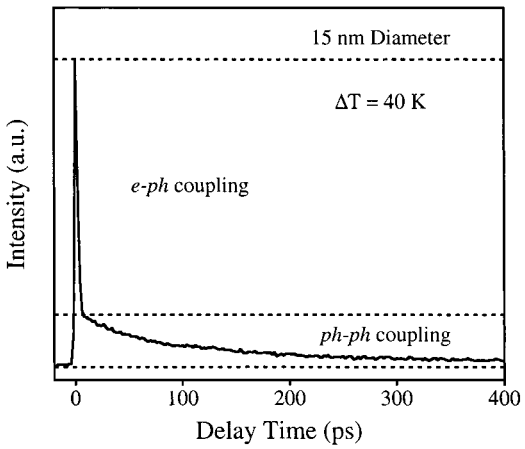

Figure 2. Transient bleach data for 15 nm diameter Au particles recorded with 530 nm probe pulses and a pump laser power of 0.4 μJ/pulse. The different regions of the decay (coupling between the electrons and phonons within the particles and coupling between the particles and their environment) are labeled in the figure.

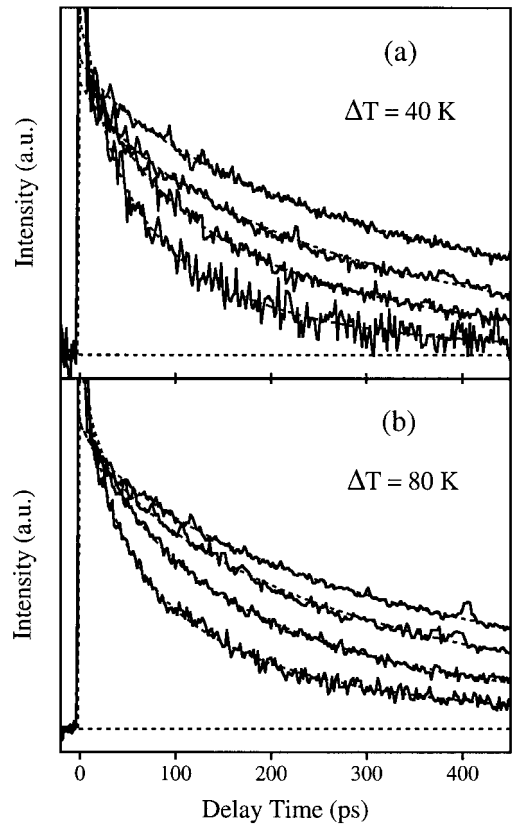

Figure 3. Transient bleach data for different sized Au particles recorded with pump laser powers of (a) 0.2 or (b) 0.4 μJ/pulses. The different traces correspond, from top to bottom, to particles with diameters of 50, 40, 26, or 15 nm. The initial temperature rise induced by the pump laser is included in the figure. The dashed lines show fits to the data using eq 3.

experiments were either 0.2 μJ per pulse (Figure 3a) or 0.4 μJ per pulse (Figure 3b). The data have been normalized by the break point between the e−ph and ph−ph coupling regions of the decay. Data from the ~4 nm diameter particles is not presented here for clarity, see Figure 6 below. Note that in general the magnitude of the bleach depends on the sample concentration, the particle size (through the intensity of the plasmon band), and the electron temperature. Normalizing by

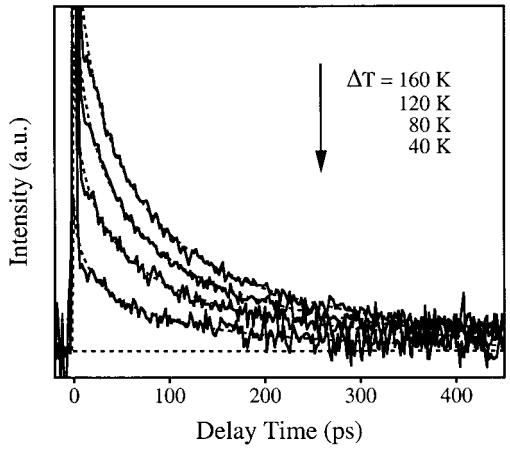

Figure 4. Transient bleach data for 15 nm diameter Au particles recorded with pump powers of 0.2, 0.4, 0.6, and 0.8 μJ/pulses. The temperature rise in the particle created by the pump laser is given in the figure. The dashed lines show fits to the data using eq 3 with the values of τ and β constrained to $\tau = 40$ ps and $\beta = 0.5$ (i.e., only the amplitude was allowed to vary). These results show that the form of the decay does not depend on the initial temperature.

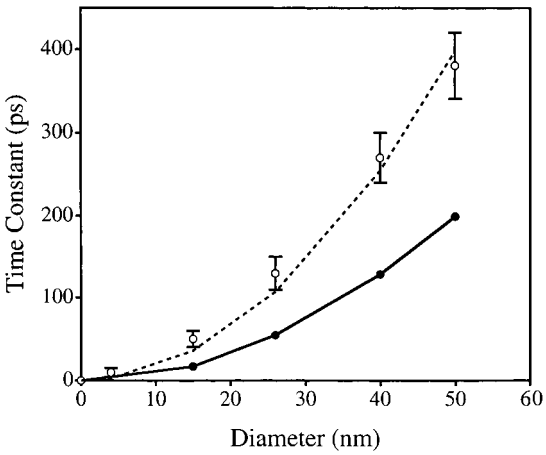

Figure 5. Characteristic time constant for energy dissipation determined using eq 3 versus diameter: (○) experimental data; (—) calculated temperature versus time profiles. The dashed line shows a fit to the data assuming a parabolic dependence of τ on diameter (i.e., $\tau \propto R^2$).

TABLE 1: Time Constants (τ) and Stretching Parameters (β) Obtained from Analysis of Experimental Transient Absorption Data and Calculated Temperature versus Time Profiles

diameter (nm)	experiment[a]		calculations	
	τ (ps)	β	τ (ps)	β
5	10 ± 5	0.6 ± 0.1		
15	50 ± 10	0.6 ± 0.1	17	0.35
26	130 ± 20	0.7 ± 0.1	55	0.40
40	270 ± 30	0.7 ± 0.1	129	0.43
50	380 ± 40	0.7 ± 0.1	199	0.44

[a] Note that the values of τ and β from the experimental data are correlated. This correlation is reflected in the reported errors.

the break point in the transient bleach decay allows us to remove the effects of the sample size and concentration from the signal and simply examine how the temperature varies for the different sized particles. Also shown in Figure 3 are fits to the transient bleach data using eq 3.

The pump laser powers used in these experiments create an initial temperature increase in the particles of $\Delta T = 40$ °C for the 0.2 μJ/pulse experiments and $\Delta T = 80$ °C for the 0.4 μJ/pulse experiments, once the electrons and phonons have reached equilibrium. These temperatures are indicated in Figure 3. Note that the amplitude of the bleach signal at the break point is linearly proportional to pump laser power. Equation 1 shows that the temperature increase in the particles is also proportional to the pump intensity, which implies that the signal in these experiments directly tracks the temperature of the particles. The results in Figure 3 show that, similar to the calculations, the characteristic time scale for energy dissipation increases as the particle size increases. In addition, for particles of the same size, the form of the bleach recovery is very similar for experiments performed at different laser powers (i.e., Figure 3 part a compared to part b). This is shown in Figure 4, where data for the 15 nm diameter particles is plotted for different pump laser powers. Fits to the data using eq 3 are also presented. The values of the time constant and stretching parameter used in these fits are identical for the four traces ($\tau = 40$ ps and $\beta = 0.5$), and only the amplitude was varied. Clearly, each trace can be well fitted using the same τ and β values; that is, the characteristic time scale for energy dissipation is the same for each laser power. Again, this result is consistent with the calculations using the general formula presented in ref 13. The amplitude extracted from the data is proportional to the laser power (which determines the initial temperature of the particles). This result is consistent with our assumption that the bleach signal is proportional to the temperature of the particles.

The values of the time constant τ obtained from fitting the experimental results in Figure 3 are plotted in Figure 5, along with the results from the calculations described above. The values of τ and β obtained from this analysis are also collected in Table 1. The dashed line in Figure 5 is a fit to the experimental time constants assuming that $\tau = \gamma R^2$. Specifically, we find that $\gamma = 0.159 \pm 0.001$ ps/nm^2, which means that the temperature in the particles at time t can be estimated by

$$\frac{T(t) - T_0}{T_i - T_0} = \exp\{-(t/0.159 \times R^2)^{0.7}\} \qquad (4)$$

where T_i is the initial temperature, T_0 is the temperature of the surroundings, and t and R are expressed in ps and nm, respectively. It is important to remember that eq 4 is purely phenomenological, there is no fundamental reason heat dissipation should follow a stretched exponential function.

The trends for the experiments and the calculations are in reasonable agreement. They both show that the characteristic time scale for energy dissipation is proportional to the surface area of the particles but does not depend on the initial temperature of the system. However, the time constants obtained from the calculations are consistently faster than those determined from the experiments. We believe that this is due to the boundary conditions used in the calculations. Specifically, in the calculations the particle and the surroundings have the same temperature at the interface. This assumption is necessary for solving the heat transfer equations for the particle/solvent system. However, it imposes the condition that energy exchange between the gold atoms in the particle and the molecules at the interface is instantaneous. For small particles, the molecular nature of the interface will be important, and this assumption must break down. Thus, the calculations effectively yield an upper bound for the rate of energy dissipation. A correct treatment of the energy transfer process will require a molecular description of the interaction between gold and the solvent.[35]

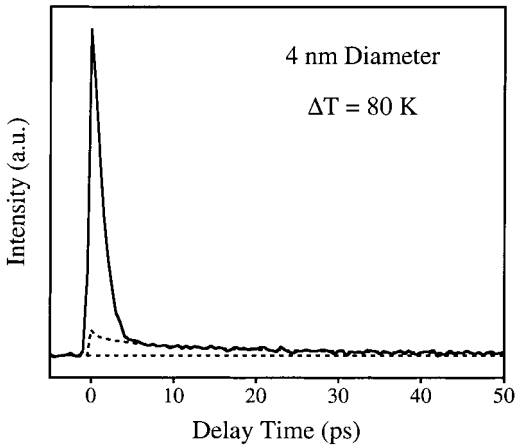

Figure 6. Transient bleach data for the 4 nm diameter particles recorded with 0.4 μJ pump laser pulses. The dashed line shows a fit to the data using eq 3. The characteristic time scale for energy relaxation obtained from this fit is $\tau = 10 \pm 5$ ps.

Figure 6 shows experimental data for the small (4 nm diameter) Au particles recorded with 0.4 μJ energy pump laser pulses. In this case, the signal is almost completely dominated by the e−ph relaxation. A fit to the data yields an estimate of the characteristic time scale for ph−ph coupling of 10 ps. This time constant is comparable to that for the e−ph coupling process (several picoseconds for this experiment). Thus, these results show that significant energy dissipation can occur before the electrons and phonons have reached equilibrium. In other words, for very small particles, the solvent molecules may interact with nonthermal electrons. Experiments are currently underway to see if these interactions can lead to unusual chemistry at the surface of small particles.

Summary and Conclusions

The experiments presented above show that the rate of energy dissipation for Au nanoparticles in aqueous solution depends on size: small particles have faster relaxation times because of their larger surface-to-volume ratios. The relaxation times do not depend on the initial temperature of the system, a surprising result that is consistent with calculations of the expected cooling times for Au particles in water.[13] The calculated time scales are consistently faster than the experimental results. This is attributed to the assumptions used in the calculations. Specifically, that the temperatures of the gold and the solvent are equal at the interface, which implies that energy exchange at the interface is instantaneous. For very small particles (~4 nm diameter), the time scale for energy dissipation (~10 ps) is comparable to the time scale for e−ph coupling (several ps). This implies that significant energy transfer to the environment can occur before the electrons and phonons have reached equilibrium. These results form an important step in our efforts to understand laser induced heating effects in metal nanoparticles.

Acknowledgment. The work described in this paper was supported by the National Science Foundation through Grant No. CHE98-16164.

References and Notes

(1) Zhang, J. Z. *Acc. Chem. Res.* **1997**, *30*, 423.
(2) Link, S.; El-Sayed, M. A. *J. Phys. Chem. B* **1999**, *103*, 8410.
(3) Hodak, J. H.; Henglein, A.; Hartland, G. V. *J. Phys. Chem. B* **2000**, *104*, 9954.
(4) Voisin, C.; Del Fatti, N.; Christofilos, D.; Vallee, F. *J. Phys. Chem. B* **2001**, *105*, 2264.
(5) El-Sayed, M. A. *Acc. Chem. Res.* **2001**, *34*, 257.
(6) Tas, G.; Maris, H. J. *Phys. Rev. B* **1994**, *49*, 15046.
(7) Hohlfeld, J.; Wellershoff, S.-S.; Güdde, J.; Conrad, U.; Jähnke, V.; Matthias, E. *Chem. Phys.* **2000**, *251*, 237.
(8) Hodak, J. H.; Henglein, A.; Giersig, M.; Hartland, G. V. *J. Phys. Chem. B* **2000**, *104*, 11708.
(9) Roberti T. W.; Smith, B. A.; Zhang, J. Z. *J. Chem. Phys.* **1995**, *102*, 3860.
(10) Ahmadi, T. S.; Logunov, S. L.; El-Sayed, M. A. *J. Phys. Chem.* **1996**, *100*, 8053.
(11) Mohamed, M. B.; Ahmadi, T. S.; Link, S.; Braun, M.; El-Sayed, M. A. *Chem. Phys. Lett.* **2001**, *343*, 55.
(12) Link, S.; Furube, A.; Mohamed, M.; Asahi, T.; Masuhara, H.; El-Sayed, M. A. *J. Phys. Chem. B* **2002**, *106*, 945
(13) Cooper, F. *Int. J. Heat Mass Transfer* **1977**, 991.
(14) Voisin, C.; Del Fatti, N.; Christofilos, D.; Vallee, F. *Appl. Surf. Sci.* **2000**, *164*, 131.
(15) Kamat, P. V.; Flumiani, M.; Hartland, G. V. *J. Phys. Chem. B* **1998**, *102*, 3123.
(16) Takami, A.; Kurita, H.; Koda, S. *J. Phys. Chem. B* **1999**, *103*, 1226.
(17) Chang, S. S.; Shih, C. W.; Chen, C. D.; Lai, W. C.; Wang, C. R. C. *Langmuir* **1999**, *15*, 701.
(18) Link, S.; Burda, C.; Nikoobakht, B.; El-Sayed, M. A. *J. Phys. Chem. B* **2000**, *104*, 6152.
(19) Link, S.; El-Sayed, M. A. *J. Chem. Phys.* **2001**, *114*, 2362.
(20) Huttmann, G.; Birngruber, R. *IEEE J. Sel. Top. Quantum Electron.* **1999**, *5*, 954.
(21) Francois, L.; Mostafavi, M.; Belloni, J.; Delaire, J. A. *Phys. Chem. Chem. Phys.* **2001**, *3*, 4965.
(22) Battaglin, G.; Calvelli, P.; Cattaruzza, E.; Polloni, R.; Borsella, E.; Cesca, T.; Gonella, F.; Mazzoldi, P. *J. Opt. Soc. Am. B* **2000**, *17*, 213.
(23) Enüstün, B. V.; Turkevich J. *J. Am. Chem. Soc.* **1963**, *85*, 3317.
(24) Henglein, A.; Meisel, D. *Langmuir* **1998**, *14*, 7392.
(25) Henglein, A. *Langmuir* **1999**, *15*, 6738.
(26) Del Fatti, N.; Voisin, C.; Chevy, F.; Vallee, F.; Flytzanis, C. *J. Chem. Phys.* **1999**, *110*, 11484.
(27) Hodak, J. H.; Henglein, A.; Hartland, G. V. *J. Chem. Phys.* **1999**, *111*, 8613.
(28) Hartland, G. V. *J. Chem. Phys.* **2002**, *116*, 8048.
(29) Logunov, S. L.; Ahmadi, T. S.; El-Sayed, M. A.; Khoury, J. T.; Whetten, R. L. *J. Phys. Chem. B* **1997**, *101*, 3713.
(30) Hodak, J. H.; Martini, I.; Hartland, G. V. *J. Phys. Chem. B* **1998**, *102*, 6958.
(31) Liz-Marzan, L. M.; Mulvaney, P. *New J. Chem.* **1998**, *22*, 1285.
(32) Kakac, S.; Yenev, Y. *Heat Conduction*; Taylor and Francis: Washington, DC, 1993.
(33) *American Institute of Physics Handbook*, 3rd ed.; McGraw-Hill: New York, 1972.
(34) *CRC Handbook of Chemistry and Physics*, 82nd ed.; CRC Press: Boca Raton, FL, 2001.
(35) Dou, Y.; Zhigilei, L. V.; Winograd, N.; Garrison, B. J. *J. Phys. Chem. A* **2001**, *105*, 2748.